Journal of Sound and Vibration (1998) **210**(4), 517–527

AN ALTERNATIVE FEEDBACK STRUCTURE FOR THE ADAPTIVE ACTIVE CONTROL OF PERIODIC AND TIME-VARYING PERIODIC DISTURBANCES

M. BOUCHARD

Mechanical Engineering Department (*G.A.U.S.*)

AND

B. PAILLARD

Electrical and Computer Engineering Department, *University of Sherbrooke*, *Sherbrooke*, *Québec*, *Canada J1K 2R1*

(*Received* 31 *January* 1997, *and in final form* 9 *September* 1997)

An alternative feedback structure, inspired from a speech coding structure, is introduced for the adaptive active control of periodic and time-varying periodic disturbances. The new structure is an Internal Model Control (IMC) structure. It separates the information and the processing pertaining to the plant from the information and the processing pertaining to the disturbance signal. A non-causal filter modelling the inverse of the secondary path is used, and the future samples of the disturbance signal are estimated by linear prediction (using an LMS algorithm). No filtering of a reference signal with the model of the secondary path is required to compute a filtered reference signal. In consequence, for the cases presented in the paper, the new feedback structure has a much faster convergence behavior and a better transient response than the classical FX-LMS algorithm with a feedback IMC structure, or the more recent and usually faster ANC-LMS algorithm with the same IMC structure. Simulation results with experimentally measured primary and secondary paths of a beam are presented, showing that either for multi-harmonic disturbance signals or sweeping sine wave disturbances, the structure presented in this paper greatly improves the convergence behavior of an adaptive feedback controller.

1. INTRODUCTION

There has been a lot of previous work on feedback active control. Some of this work was on non-adaptive feedback controllers [1–6]. This paper is concerned with the control of periodic and time-varying periodic disturbance signals, and in this case, fixed feedback controllers are not appropriate. For example, fixed broadband feedback controllers are adjusted to provide a medium attenuation over a broad frequency range. They often can not do much better than to "flatten" sharp resonances in the transfer function of the primary path, so they can't produce a large attenuation (say 25–30 dB) of one or more sine waves sweeping over a large frequency band. On the contrary, an adaptive "tonal" controller (with very few coefficients) can achieve a good reduction of several sine waves sweeping over the whole frequency range. It does so by creating and sliding "notches" in the frequency response of the sensitivity function. The most popular adaptive feedback structure used in active control today is probably the Internal Model Control structure (IMC) [7], combined with a stochastic gradient descent algorithm such as the FX-LMS [8]. Figure 1 illustrates this structure. More recently, a modification to the FX-LMS

0022–460X/98/090517 + 11 $25.00/0/sv971297

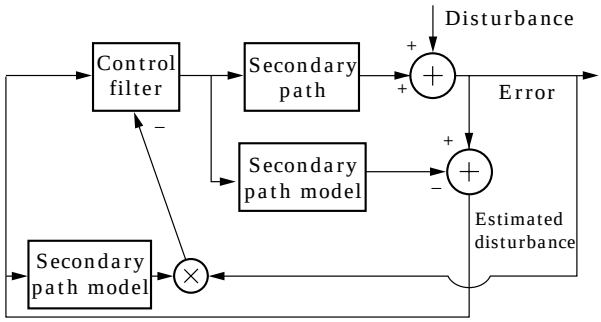

Figure 1. Block diagram of the FX-LMS algorithm using the feedback IMC structure.

algorithm was proposed to eliminate the dependency of the step size used in the algorithm, to the delay of the secondary path [9]. The resulting structure is illustrated in Figure 2, and the algorithm will be called ANC-LMS in this paper.

For feedback control using an IMC structure, both the FX-LMS and the ANC-LMS require the filtering of the estimated disturbance signal with a model of the secondary path, to generate the filtered reference signal. This leads to two problems. First, the statistics of the filtered reference signal may be very different from the statistics of the original disturbance signal. This is true in particular for secondary paths with large spectral dynamics. For example, in the case of a multi-harmonic disturbance, it is possible that some energetic tones in the disturbance signal are not well represented (energetic) in the filtered reference signal. As a result, adaptation for those tones is slow, and a slow global convergence is observed. Secondly, for secondary paths with low damping, the impulse response is long and it causes a large delay in the generation of the filtered reference signal. This leads to a slow convergence or a bad transient response (overshoot), in particular in the case of time-varying disturbance signals, as it will also be shown in this paper.

Feedback approaches that do not require the filtering with the secondary path have been developed for adaptive active controllers. A feedback waveform synthesis method was introduced in reference [10]. This approach requires synchronous sampling with a fundamental disturbance frequency, which is not always practical. Another adaptive method called the output whitening feedback was proposed in references [11, 12]. This method performs well if the secondary path is minimum phase, but it is often not the case

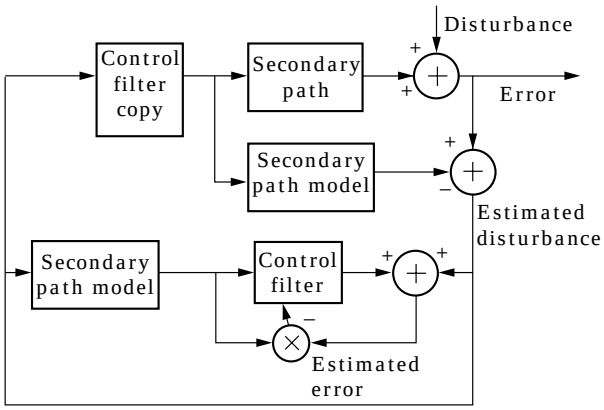

Figure 2. Block diagram of the ANC-LMS algorithm using the feedback IMC structure.

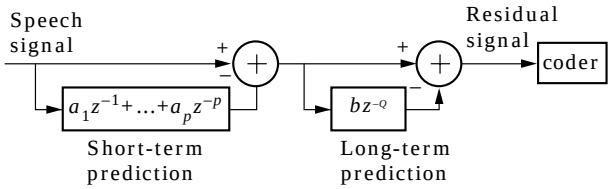

Figure 3. Block diagram of a prediction structure in low-bit rate speech coding.

in many situations, like in the secondary path used in this paper. Another method was developed by Oppenheim *et al*. [13], which uses Kalman filtering and assumes that the secondary path is a pure delay. However, secondary paths are rarely pure delays, such as the secondary path considered in this paper.

A new adaptive feedback active control structure is introduced, which also uses the IMC structure to estimate the disturbance signal. However, the new feedback structure does not require the filtering of the reference signal (the estimated disturbance signal in this case) with the model of the secondary path. For the practical control problem considered in this paper (the active control of the vibrations of a beam), this greatly improves the convergence of the new feedback structure, compared to the FX-LMS and ANC-LMS algorithms using IMC structures. The applicability of the new structure is mainly for periodic or time-varying periodic disturbances.

In the next section, the new adaptive feedback control structure is developed. It will be called the ''inverse feedback structure''. In section 3, simulation results are presented, comparing the behavior of the FX-LMS and ANC-LMS algorithms with the IMC feedback structure, and the inverse feedback structure with an LMS algorithm as the predictor. Section 4 briefly comments on the computational loads of the three different structures and algorithms discussed in this paper.

2. DEVELOPMENT OF THE INVERSE FEEDBACK STRUCTURE

In most low bit-rate coding schemes for speech coding, a separate long-term and short-term prediction is used to reduce the redundancy (predictability and coherence) of the ''voiced'' speech signal to be coded (Figure 3). The short term prediction is used to model the vocal track of the speaker, and the long term prediction is used to predict the ''pitch'' (fundamental period) of the physiological signal that excites the vocal track [14]. The concept of separating the information and the processing pertaining to the vocal track (the plant), from the information and the processing pertaining to the excitation signal, can also be brought to the field of active control of noise and vibration.

An approach has already been published [1], in which a feedback controller is conceptualized in two parts : a compensator and a regulator (Figure 4). In that paper, the feedback controller is not using an IMC structure. The compensator filter is the inverse

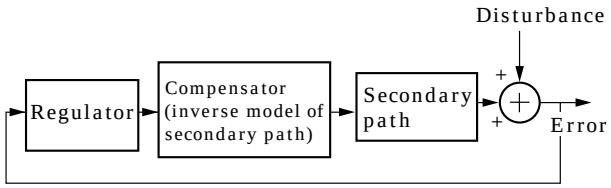

Figure 4. Block diagram of a feedback controller with two parts: a regulator and a compensator.

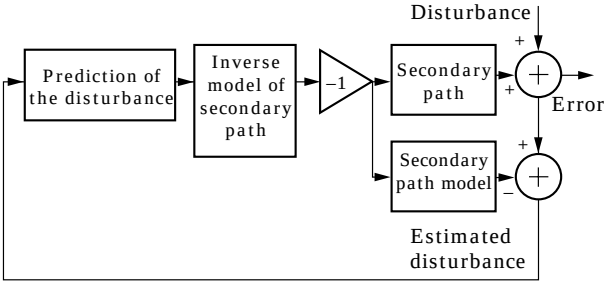

Figure 5. Block diagram of an IMC feedback controller with two parts: a predictor and a compensator (inverse model).

of the secondary path, and the regulator is a filter which has a high gain over the frequency band in which reduction is sought. The cascade of the compensator and the regulator is assumed to be causal in reference [1]. In the case of the IMC feedback structure, it is similarly possible to conceptualize the feedback controller in two parts : one part is the (non-causal) inverse of the secondary path, and the other part is the predictor of the disturbance (Figure 5). With the IMC control structures of Figures 1 and 2, for a time-varying periodic disturbance signal, the control filter takes into account both the inverse of the secondary path and the prediction of the disturbance. On the contrary, with the structure of Figure 5, the inverse of the secondary path and the prediction of the disturbance are separately performed. The time constants of the variations of the secondary path are usually much longer than the time constants of the disturbance fluctuations. The adaptation effort can then be put on the prediction of the disturbance, and the inverse of the secondary path can be considered constant over a certain amount of time.

In feedback control, only the causal inverse of the secondary path is usually considered [15]. This is because non-causal control filters require the knowledge of the future samples of the disturbance signal or the error signal, which are usually unknown. However, since this paper is concerned with the control of periodic or time-varying periodic disturbance signals, the future samples of the disturbance signal can be predicted, and the non-causality of the inverse filter of the secondary path is not a problem. In this paper, the inverse filters that will be used will be non-causal if the secondary path is non minimum phase or has a delay. To predict the future samples of the disturbance signal, a simple LMS predictor can be used. Figure 6 shows a block diagram of the resulting feedback control structure; hereafter, this structure will be referred to as the ''inverse feedback structure''.

The approach of predicting the future components of the disturbance signal could also be applied for narrowband disturbance signals. However, in the structure of Figure 6, the signal that is sent to the model of the inverse secondary path ($\hat{d}(k + L)$) is built from an L steps-ahead forward prediction. L is the number of non-causal coefficients in the inverse model of the secondary path, and it should not be confused with the number of coefficients used in the predictor. In the case of a narrowband disturbance signal, if L is large, then the prediction of the disturbance signal is poor. So the inverse feedback structure is not limited to the attenuation of pure tones, but its efficiency is limited by the L steps-ahead predictability of the disturbance signal.

The transfer functions (primary and secondary paths) that are used in the simulations of the next section have been measured on a simply supported beam. This is a physical system with low damping, so it has large spectral dynamics and a long impulse response. For this physical system, two problems are observed when using the filtered-X approaches

(FX-LMS and ANC-LMS). As mentioned in the introduction, with the filtered-X approaches, the statistics of the filtered reference signal may be very different from the statistics of the original disturbance signal. For the case of the feedback control of a multi-harmonic disturbance (presented in the next section), this leads to a situation where some energetic tones in the disturbance signal are not well represented (energetic) in the filtered reference signal. Consequently, convergence is slow on those components, and global convergence is slow. The inverse feedback structure does not have this problem.

Secondly, since the impulse response of the secondary path is long for the considered physical system, it causes a large delay in the generation of the filtered reference signal. This leads to a slow convergence and a bad transient response (overshoot) in the case of the feedback control of a sweeping sine disturbance, as presented in the next section. The inverse feedback structure performs better in this case because the impulse response of the inverse of the secondary path is much shorter than the impulse response of the secondary path itself.

There are also some other advantages of using the inverse feedback structure. There is the availability of an advanced error criterion (the prediction error in Figure 6), that could eventually be used to temporarily turn off the controller in time, for situations where it can't perform well. This advanced error criterion is not used in this paper. Also, if the disturbance signal is composed of broadband components as well as periodic (tonal) components, then the inverse feedback structure still performs well on the tonal components, since only the predictable (tonal) components of the disturbance signal are filtered by the model of the inverse secondary path. The broadband "noisy" components are thus implicitly eliminated from the signal sent to the control actuator.

There is, however, a disadvantage in using the inverse feedback structure. Indeed, any imprecision in the modelling of the secondary path (for the IMC structure) and the modelling of the inverse of the secondary path, may reduce the control attenuation produced by the controller. In other words, the information from the error signal (Figure 6) is not used by the structure to adapt the controller. On the contrary, the

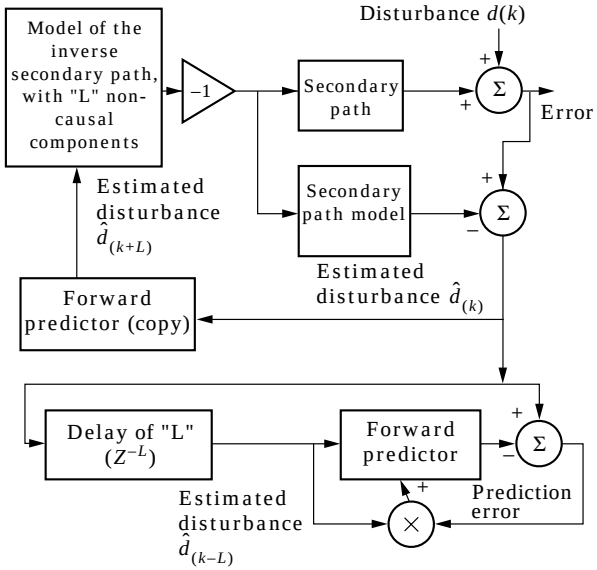

Figure 6. Detailed block diagram of the inverse feedback structure ("L" is the number of non-causal components in the model of the inverse secondary path).

TABLE 1

Computational loads of the different algorithms and structures

Structure and algorithm	Computational load (no. multiplications/additions)
IMC structure with FX-LMS	$2M + 2N$
IMC structure with ANC-LMS	$3M + 2N$
Inverse feedback structure with LMS predictor	$N + P + 3R$

FX-LMS and ANC-LMS algorithms can compensate up to a certain point for the imprecision on the model of the secondary path, because those algorithms use the feedback information from the error signal. It is well known for feedforward controllers that if slow convergence is acceptable, a tonal FX-LMS controller can compensate for a phase error up to 90° in the model of the secondary path [16]. This is certainly not the case for the inverse feedback structure.

In Table 1, the computational loads (number of multiplications/additions) of the FX-LMS with the IMC structure, the ANC-LMS with the IMC structure, and the inverse feedback structure with a LMS predictor are presented. In the table, M is the number of coefficients for the adaptive control filter of the FX-LMS and the ANC-LMS, N is the number of coefficients for the model of the secondary path, P is the number of coefficients for the model of the inverse of the secondary path, and R is the number of coefficients for the LMS predictor in the inverse feedback structure. Typically, if the number of coefficients in the model of the secondary path is larger than the number of coefficients in the model of the inverse secondary path, then the inverse feedback structure has a lower computational load (neglecting M and R that are usually small for tonal controllers). If it is not the case, then the inverse feedback structure has a higher computational load. But in all cases, the computational loads are usually of the same order of magnitude.

3. SIMULATIONS OF FEEDBACK CONTROL

In this section, simulations compare the convergence behavior of the FX-LMS and ANC-LMS algorithms using feedback IMC structures with the inverse feedback structure using a LMS predictor. Normalized versions of the algorithms are used, so the algorithms could also be called FX-NLMS controller, ANC-NLMS controller and inverse feedback with NLMS predictor. The simulated control structures are identical to those illustrated in Figures 1, 2 and 6, with the addition of a primary path between the disturbance source and the disturbance signal. Care was taken so that all the transients related to the start of the simulating process were completely propagated in the system, before turning on a controller. In all cases, the optimal step size for each algorithm was found by trial and error. As mentioned earlier, primary and secondary paths were experimentally measured as the vibration response of a beam (with PZT actuators and a PVDF sensor), and the impulse response and frequency response of those paths are illustrated in Figures 7 and 8.

The inverse feedback structure needs a model of the inverse of the secondary path. That inverse model can be identified directly from actuator and error sensor signals, or it can be computed using the (direct) measured model of the secondary path. The latter approach was used in this paper. Figure 9 shows an inverse model of the secondary path that uses only 128 coefficients (64 non-causal coefficients and 64 causal coefficients). A better precision could be obtained by using more coefficients, but this 128-coefficient inverse

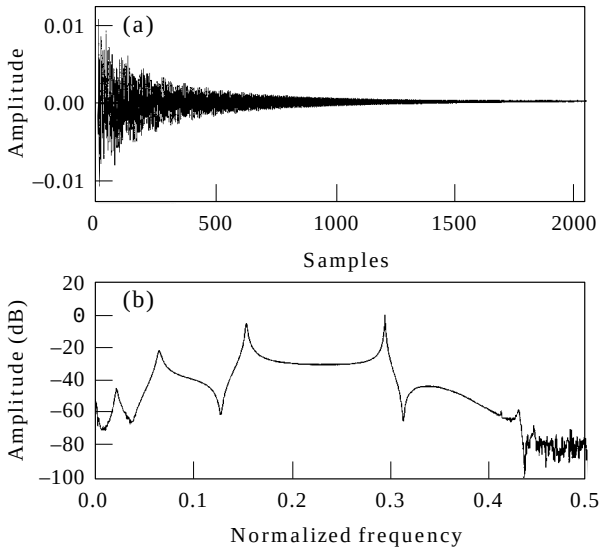

Figure 7. (a) Impulse response and (b) frequency response of the primary path.

model will be used for two reasons. First, it provides enough precision to obtain 25–30 dB of reduction on most periodic or time-varying periodic disturbance signals. Second, the fact that the inverse model is shorter than the model of the secondary path (Figure 8) improves the convergence of the inverse feedback structure with time-varying disturbance signals.

Two disturbance sources have been simulated: a fixed multi-harmonic source, and a sweeping sine wave source. The multi-harmonic case is considered first. In this case, the fundamental frequency was chosen so that one of the harmonics is close to a resonance frequency of the secondary path. Figures 10 and 11 show the power spectrum of the

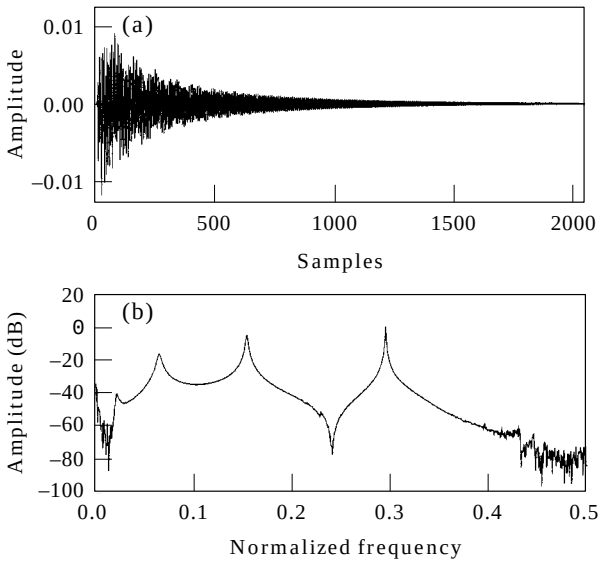

Figure 8. (a) Impulse response and (b) frequency response of the secondary path.

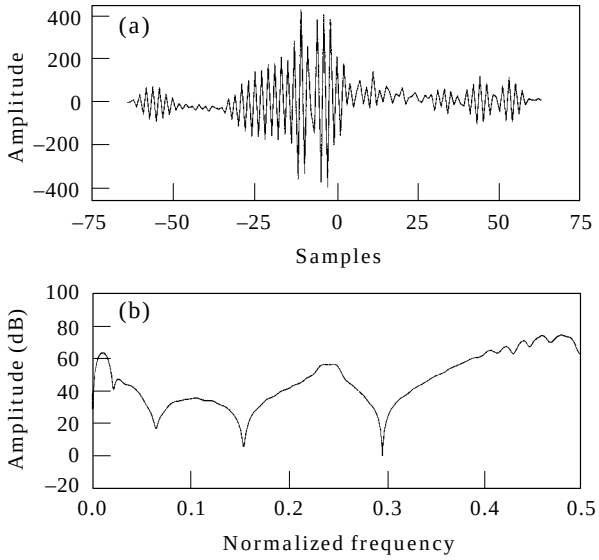

Figure 9. (a) Impulse response and (b) frequency response of the 128-coefficient model of the inverse secondary path.

disturbance source and the disturbance signal, respectively. The FX-LMS and ANC-LMS algorithms produce a filtered reference signal, in this case computed by filtering the disturbance signal with the model of the secondary path. The power spectrum of that filtered reference signal is shown in Figure 12, where it can be observed that the highest frequency harmonic is much more energetic than the other harmonics in the filtered reference signal. It can thus be predicted that a fast convergence will only be observed for that highest frequency harmonic with the FX-LMS and ANC-LMS algorithms.

Figure 13 shows the convergence behavior of the three approaches considered. Twelve coefficients were used for the control filter with the FX-LMS and ANC-LMS algorithms, and 12 coefficients were also used for the LMS predictor in the inverse feedback structure. Normalized step sizes were 1·0 (0 dB) for the ANC-LMS algorithm and the inverse

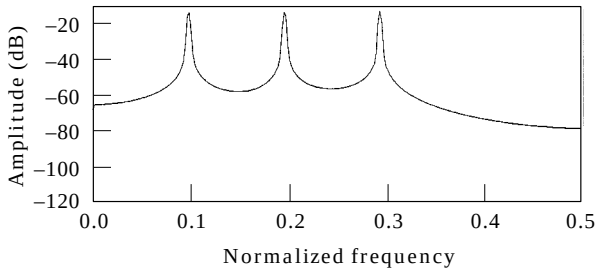

Figure 10. Power spectrum of the disturbance source.

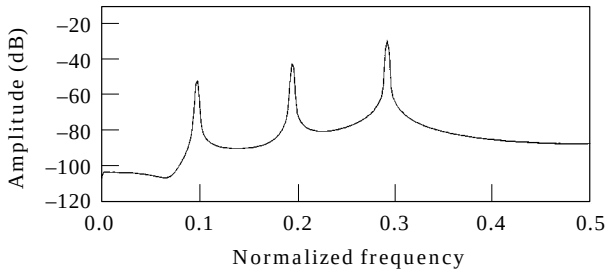

Figure 11. Power spectrum of the disturbance signal.

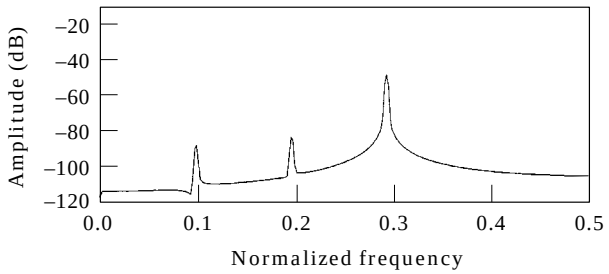

Figure 12. Power spectrum of the filtered reference signal.

feedback LMS predictor, and 0·00398 (-24 dB) for the FX-LMS algorithm. It can be seen in Figure 13 that both the FX-LMS and the ANC-LMS algorithms exhibit a slow global convergence behavior in this case. The convergence speed of the inverse feedback structure is much faster. The performance of the inverse feedback structure is, however, limited to a 30-dB attenuation because of the limited precision (small number of coefficients used) in the model of the inverse secondary path. Eventually, after many iterations, the FX-LMS and the ANC-LMS will also produce over 30 dB of attenuation, and even more since they do not have the limitation on the precision of the inverse model. Figure 14 shows the power spectrum of the error signal in the case of the ANC-LMS algorithm, after more than 5000 iterations of convergence. It clearly appears that only the highest frequency harmonic is quickly reduced with a filtered-X approach.

Simulation results with a sweeping sine wave disturbance source are now presented. The sine wave sweeps from a normalized frequency of 0·1 cycle/sample to a normalized frequency of 0·2 cycle/sample, at a rate of 0·0002 (cycle/sample)/sample. The sweeping process thus lasts 500 samples. For example, this would correspond to a 1-s transition from

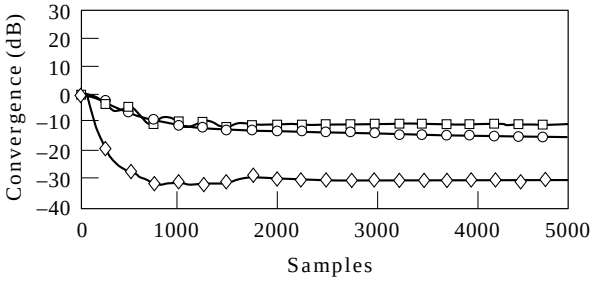

Figure 13. Convergence behavior of the FX-LMS algorithm, □; the ANC-LMS algorithm, ○; and the inverse feedback structure with an LMS predictor, ◇.

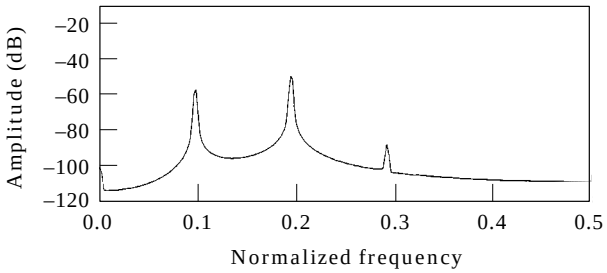

Figure 14. Power spectrum of the error signal after more than 5000 iterations, ANC-LMS algorithm.

a 50 Hz (3000 r.p.m.) pure tone to 100 Hz (6000 r.p.m.) pure tone at a rate of 50 Hz/s (3000 r.p.m/s), for a 500-Hz sampling frequency. It should be noted that the frequency of the sweeping sine wave will pass through a resonance frequency in both the primary path and the secondary path (Figures 7 and 8). In the simulation, the disturbance source waits 4500 samples after the 500 samples of sweeping, before sweeping back from the normalized frequency of 0·2 cycle/sample to the 0·1 cycle/sample frequency. The whole process lasts 10 000 samples, and Figure 15 presents the convergence behavior of the different control structures and algorithms over this period of 10 000 samples. Four coefficients were used for the control filter with the FX-LMS and ANC-LMS algorithms, and four coefficients were also used for the LMS predictor in the inverse feedback structure. Normalized step sizes were 0·0158 (−18 dB) for the FX-LMS, the ANC-LMS and the LMS (predictor) algorithms. This was the optimal step size for all algorithms. Using a higher step size was causing a larger overshoot and did not accelerate the convergence speed. It is clear from Figure 15 that the inverse feedback structure with an LMS predictor exhibits a faster convergence behavior and produces less overshoot than the other two approaches. The attenuation of the inverse feedback structure is limited to about 25 dB, again because of the small number of coefficients used in the model of the inverse secondary path. The steady-state attenuation produced by the other algorithms is however better than 25 dB.

4. CONCLUSION

A new adaptive feedback structure suited for the active control of periodic or time-varying periodic disturbance signals is presented. The new approach does not require the filtering of the disturbance signal with the model of the secondary path. Simulations from experimentally measured transfer functions showed that this can improve the

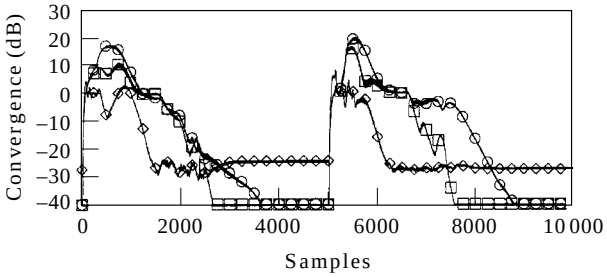

Figure 15. Convergence behavior of the FX-LMS algorithm, □; the ANC-LMS algorithm, ○; and the inverse feedback structure with a LMS predictor, ◇.

convergence behavior of the proposed structure, over the convergence behavior of the IMC structure combined with the FX-LMS algorithm, or the usually faster ANC-LMS algorithm. The computational load of the proposed structure is often similar or lower to the computational load of the FX-LMS (or the ANC-LMS) using a feedback IMC structure.

ACKNOWLEDGMENTS

Financial support for this work was provided by the "Institut de Recherche en Santé et Sécurité au Travail" (I.R.S.S.T.).

REFERENCES

1. E. F. Berkman and E. K. Bender 1997 *Journal of Sound and Vibration* **31**, 80–94. Perspectives on active noise and vibration control.
2. P. D. Wheeler and D. Smeatham 1992 *Applied Acoustics* **36**, 159–162. On spatial variability in the attenuation performance of active hearing protectors.
3. J. Thi and D. R. Morgan 1992 *Proceedings of the International Conference on Acoustics*, *Speech and Signal Processing*, Vol. II, 233–236. A broadband pseudo-cascade active control system.
4. J. L. Dohner and R. Shoureshi 1989 *Journal of Vibrations*, *Acoustics*, *Stress*, *and Reliability in Design* **111**, 326–330. Modal control of acoustics plants.
5. M. H. Costin and D. R. Elzinga 1989 *IEEE Control Systems Magazine* **9**, 3–6. Active reduction of low-frequency tire impact noise using digital feedback control.
6. W. K. W. Hong, K. Eghtesadi and H. G. Leventall 1987 *Journal of the Acoustical Society of America* **81**, 376–388. The tight-couple monopole (TCM) and tight-couple tandem (TCT) attenuators: theoretical aspects and experimental attenuation in an air duct.
7. M. Morari and E. Zafiriou 1989 *Robust Process Control*. Englewood Cliffs, NJ: Prentice Hall.
8. S. J. Elliott and P. A. Nelson 1993 *IEEE Signal Processing Magazine* **10**, 12–35. Active noise control.
9. I. S. Kim, H.-S. Na, K.-J. Kim and Y. Park 1994 *Journal of the Acoustical Society of America* **95**, 3379–3389. Constraint filtered-x and filtered-u least-square algorithms for the active control of noise in ducts.
10. G. B. B. Chaplin and R. A. Smith 1986 *U. S. Patent* 4,566,118. Method and apparatus for canceling vibration from a source of repetitive vibrations.
11. A. J. Efron and L. C. Han 1994 *IEEE Transactions on Circuits Systems II*, *Analog Digital Signal Process*. **41**, 405–409. Wide-area adaptive active noise cancellation.
12. D. Graupe and A. F. Efron 1991 *IEEE Transactions on Circuits Systems* **38**, 1306–1313. An output-whitening approach to adaptive active noise cancellation.
13. A. V. Oppenheim, E. Weinstein, K. C. Zangi, M. Feder and D. Gauger 1994 *IEEE Transactions on Speech Audio Processing* **2**, 285–290. Single-sensor active noise cancellation.
14. N. Moreau 1995 *Techniques de Compression des Signaux*. Paris: Masson.
15. B. Widrow and E. Walach 1996 *Adaptive Inverse Control*. Englewood Cliffs, NJ: Prentice Hall.
16. C. C. Boucher, S. J. Elliott and P. A. Nelson 1991 *IEE Proceedings of F. Radar Signal Processing* **138**, 313–319. Effect of errors in the plant model on the performance of algorithms for adaptive feedforward control.